FULL PAPER

Temporal Modulation of Stem Cell Activity Using Magnetoactive Hydrogels

*Amr A. Abdeen, Junmin Lee, N. Ashwin Bharadwaj, Randy H. Ewoldt, and Kristopher A. Kilian**

Cell activity is coordinated by dynamic interactions with the extracellular matrix, often through stimuli-mediated spatiotemporal stiffening and softening. Dynamic changes in mechanics occur in vivo through enzymatic or chemical means, processes which are challenging to reconstruct in cell culture materials. Here a magnetoactive hydrogel material formed by embedding magnetic particles in a hydrogel matrix is presented whereby elasticity can be modulated reversibly by attenuation of a magnetic field. Orders of magnitude change in elasticity using low magnetic fields are shown and reversibility of stiffening with simple permanent magnets is demonstrated. The broad applicability of this technique is demonstrated with two therapeutically relevant bioactivities in mesenchymal stem cells: secretion of proangiogenic molecules, and dynamic control of osteogenesis. The ability to reversibly stiffen cell culture materials across the full spectrum of soft tissue mechanics, using simple materials and commercially available permanent magnets, makes this approach viable for a broad range of laboratory environments.

1. Introduction

Cells adapt and respond to their local microenvironment in a context dependent fashion, that depends on spatiotemporal control of biophysical and biochemical properties.[1] The chemistry,[2] structure,[3] and mechanics[4,5] of the extracellular matrix (ECM) all influence cellular activity. This sensitivity to the environment enables cells to maintain ECM homeostasis by responding to external changes[6] and allows highly versatile stem cells to take on multiple roles in different niches.[7] This complexity, however, is significantly challenging to deconstruct with in vitro approaches when trying to decipher the properties that facilitate a specific activity or outcome.[8] Thus, the development of engineered model matrices is imperative for the study of ECM properties that guide cellular behavior.

A. A. Abdeen, J. Lee, Prof. K. A. Kilian
Department of Materials Science and Engineering
University of Illinois at Urbana–Champaign
Urbana, IL 61801, USA
E-mail: kakilian@illinois.edu
N. A. Bharadwaj, Prof. R. H. Ewoldt
Department of Mechanical Science and Engineering
University of Illinois at Urbana–Champaign
Urbana, IL 61801, USA

DOI: 10.1002/adhm.201600349

Mechanotransduction, whereby cells sense their mechanical environment and process this information into biochemical signals, is a complex process[9] that occurs ubiquitously[10] and has severe consequences when disrupted.[11] Adult mesenchymal stem cells (MSCs), due to their relevance to regenerative medicine, have been studied extensively to investigate their responsiveness to mechanical properties of the ECM. MSC fate decisions can be driven by mechanical factors such as substrate stiffness[12,13] and cell geometry.[14–16] Furthermore, the MSC secretome can be influenced by such factors, which may be used to optimize their proangiogenic therapeutic capabilities.[17,18] Interestingly, in several of these studies,[12,19,20] using physiological conditions gave optimal results.

Contrary to the polymeric cell culture substrates used in most of these studies, cellular environments are not static. In fact, the ECM is constantly changing in normal[21] and diseased[22,23] tissue. Several reports have shown that, in addition to sensing their current environment, stem cells are affected by or "remember" their mechanical history.[24–26] In addition, although great care is usually given to the temporal regulation of chemical factors used in several protocols (during somatic cell reprogramming,[27] for instance), there is no reason to assume that mechanical regulation is not just as important. In fact, a recent study utilizing tunable polymeric materials to study the effects of parameters such as anisotropic topographic cues[28] or stress relaxation[29] reveal highly dynamic cellular responses. Therefore, there is a need for in vitro cell culture platforms with externally tunable mechanical properties in order to study the temporal effect of these parameters.[30]

There have been several innovative strategies for making tunable stiffness systems. For example, pH,[31] DNA strands,[32] and calcium ion concentration[33] have been used to reversibly change substrate stiffness. However, these factors may affect cellular signaling and stiffness changes occur over different time scales. Another strategy is to alter the structure of the hydrogel using multistep crosslinking[34] (for stiffening) or controlled degradation[35] (for softening) using various methods. For example, Kloxin et al. used photodegradable hydrogels to tune the gel microenvironment through visible light irradiation.[36] Although these methods work well for one-directional changes in elasticity, they cause irreversible changes in gel structure

and do not offer reversibility. Recently, Rosales et al.[37] used an azobenzene based reversibly photoswitchable poly (ethylene glycol) (PEG) hydrogel. However, these gels can thermally relax and only show a modest change in modulus. Reversibility and the ability to modulate stiffness in a controlled manner are important to study continuous, temporally modulated changes that occur in vivo such as during development, homeostasis or disease (for example, fibrosis or wound healing)[38] or in vitro to ascertain how long it takes for changes in cell behavior to become permanent (mechanical dosing). MSCs, for instance, show irreversible changes in localization of transcriptional coactivator yes-associated protein in the nucleus by 10 d of culture in stiff conditions but these changes could be reversed by switching the environment before 10 d.[25]

In this paper, we adapt magnetorheological gels[39] and elastomers[40,41] into a magnetically tunable hydrogel platform for cell culture. We modify carbonyl iron (CI) particles for incorporation into polyacrylamide hydrogels and we demonstrate over two orders of magnitude shift in hydrogel compliance in response to magnetic fields. The gel stiffness can be easily and reversibly changed using permanent magnets, obviating the need for complex instrumentation, and thus making this technique amenable to virtually any research laboratory. Using mesenchymal stem cells as a model adult stem cell with therapeutic potential we show how magnetic fields modulate cell spreading and cytoskeletal tension, which impacts secretion of proangiogenic molecules and the propensity to undergo osteogenesis. The simplicity in which hydrogel mechanical properties can be modulated in situ will make this tool useful for a wide variety of applications, where temporal control over the biophysical microenvironment is desired.

2. Results

2.1. Gel Concept and Fabrication

We used polyacrylamide (PA) as the base polymeric hydrogel for our system, because of PA's flexibility as a cell culture platform with tunable elasticity within physiological stiffness ranges.[42] Furthermore, PA has been previously used in multiple studies with MSCs,[12,16,17,43] which provide a wealth of preliminary data for MSC behavior on soft and stiff PA substrates. These gels are formed through radical addition polymerization (**Figure 1**a) as described previously.[42]

In order to add magnetic tunability to our hydrogels, we adapted the approach of Mitsumata et al., where CI particles were incorporated into carrageenan hydrogels[39] (Figure 1b). In order to make the particles more stable in cell culture conditions, and allow functionalization of the particles, we used silane chemistry to modify the surface with different functional groups (Figure 1c, top). This has the added benefit of allowing modular modifications to the system such as covalent incorporation of moieties to the particles or the chemical crosslinking of particles into the hydrogel network. To demonstrate the efficacy of this treatment, we used two different silanes: aminopropyl triethoxysilane (APTES) to passivate the particles to stabilize them for long term cell culture, and 3-(trimethoxysilyl)-propyl-methacrylate (TMSPM) to enable covalent incorporation into PA gels. FTIR analysis shows a change in the spectrum upon treatment with APTES and TMSPM with characteristic peaks showing chemical conjugation at ≈1080 cm^{-1}, attributed to open chain siloxane groups, with the TMSPM treated particles showing characteristic peaks at ≈1638 cm^{-1} (C=C)

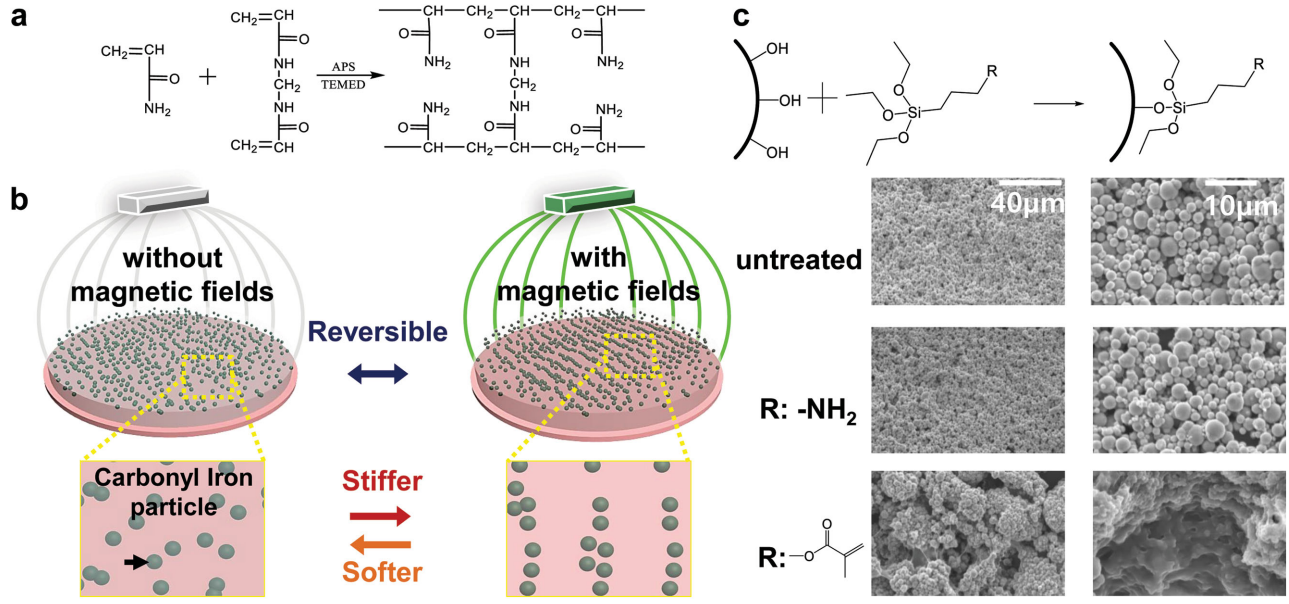

Figure 1. Carbonyl iron polyacrylamide composite hydrogel formation and stiffening. a) Formation of polyacrylamide via radical polymerization from acrylamide and bis-acrylamide monomers. b) Schematic of magnetoactive hydrogel system formed by incorporation of carbonyl iron (CI) particles in a polyacrylamide matrix. Subjecting these gels to magnetic fields causes alignment of the particles, stiffening the hydrogels.[35] c) Silane modification of CI particles. (Top) Silane chemistry can be used to modularly modify the surface of CI particles. (Bottom) SEM images of dried PA hydrogels with incorporated CI particles that are untreated, treated with an amine-terminated silane, or treated with a methacrylate terminated silane. The latter shows covalent incorporation into the hydrogel and aggregation behavior.

and 1720 cm^{-1} (C=O)[44] (Figure S1, Supporting Information). Upon incorporation of the modified particles into the hydrogels, the gels were dried and imaged using scanning electron microscopy (SEM) to see whether there was any visible effect on the structure (Figure 1c, bottom). The amine-terminated particles, while they appear similar to untreated particles in SEM, demonstrated a significant improvement in stability under prolonged cell culture conditions, where gels made with untreated particles dissolve within 10 d (Figure S2, Supporting Information). The methacrylate-terminated particles, on the other hand, show different characteristics to both amine terminated and untreated particles. SEM images show gel residues attached to the particles indicating covalent attachment of the hydrogel to the particles during gelation. An unforeseen consequence of the treatment, however, was aggregation of the particles into "clumps," presumably due to heterogeneous polymerization between monomer and particles. For all particle treatments, repeated application and removal of magnetic fields does lead to some limited leaching of particles from the hydrogel, however leached particles sediment to the bottom of well plates and do not further impact cell behavior. APTES modified particles were used for the remainder of the study unless otherwise noted.

2.2. Mechanical Characterization of Hydrogels

Shear rheometry was used to characterize the hydrogel's mechanical properties and their response to magnetic fields using a magnetorheological setup (Figure S3a, Supporting Information). The gel composite is a viscoelastic solid as observed by creep compliance and oscillatory shear measurements (Figure S3b,c, Supporting Information), with linear viscoelastic equilibrium compliance $J \approx 0.01$ Pa^{-1} (modulus $G \approx 0.1$ kPa). Figure S3b (Supporting Information) shows the strain amplitude dependence of the gel composite viscoelasticity at a frequency of 1 rad s^{-1}; the sweep range was chosen to avoid a nonlinear response that may irreversibly affect the sample. We observed almost constant storage modulus and a slowly rising loss modulus between 0.1% and 10% strain. This agrees with previous data for polyacrylamide.[45] We use a strain amplitude of 1% for performing all further linear viscoelastic measurements on the gel. Linear viscoelastic frequency sweep measurements (Figure S3c, Supporting Information) indicate minimal frequency dependence. Further information at longer timescales is obtained from a creep compliance test (Figure S3d, Supporting Information). At short times, inertioelastic oscillations are observed, due to the well-known effect of sample elasticity coupling to instrument rotational inertia. At longer times beyond 100s, the compliance $J(t)$ is nearly constant, indicating solid-like behavior at these timescales.

The gel composite dramatically stiffens in response to magnetic field, as shown in **Figure 2**. The reproducibility of the magnetic field effect is shown in Figure 2a, as observed by cycling the magnetic field between 0 and 0.75 T several times. Each full cycle was 1 min (30 s at 0 T and 30 s at 0.75 T). The storage modulus G' at 0 T ranged between 0.1 and 0.14 kPa and at 0.75 T stiffened to 60–90 kPa. The gel recovered its elastic modulus at 0 T with each cycle, indicating no irreversible disruption of the polymer network. The modulus at 0.75 T increased marginally with each cycle, but this is insignificant in the context of the relative change in moduli from 0 to 0.75 T. Importantly, this range of mechanical behavior corresponds to nearly the entire range of physiological stiffness observed in biology, from brain tissue to collagenous bone.[12] Thus, a single hydrogel can cover the entire spectrum of physiological elasticity, dynamically, and on a single gel surface.

The sensitivity to continuously modulated magnetic field strength is shown in Figure 2b, with a magnetic field ramp from 0.1 to 1 T. The elasticity (G') transitioned smoothly and continuously as the magnetic field was raised, starting to level off and saturate around 0.8 T. Magnetic saturation is a well-known effect in magnetoresponsive materials.[46] Hysteresis effects are also apparent when the magnetic field is cycled through positive and negative values (Figure 2c), with cyclic ramps from 1 to –1 T. Between cycles, the gel appeared to attain identical values of G' at 0 T, but the approach to this value depended on the direction of the field, showing signs of hysteresis in the mechanical response. When compared with cycle 1 (1 to 0 T), the gel elasticity in cycle 2 is larger in the first half of the cycle (–1 to 0 T), but smaller in the second half (0 to1 T). We attribute this to the magnetic hysteresis of the particles, which may consequently result in the particle network

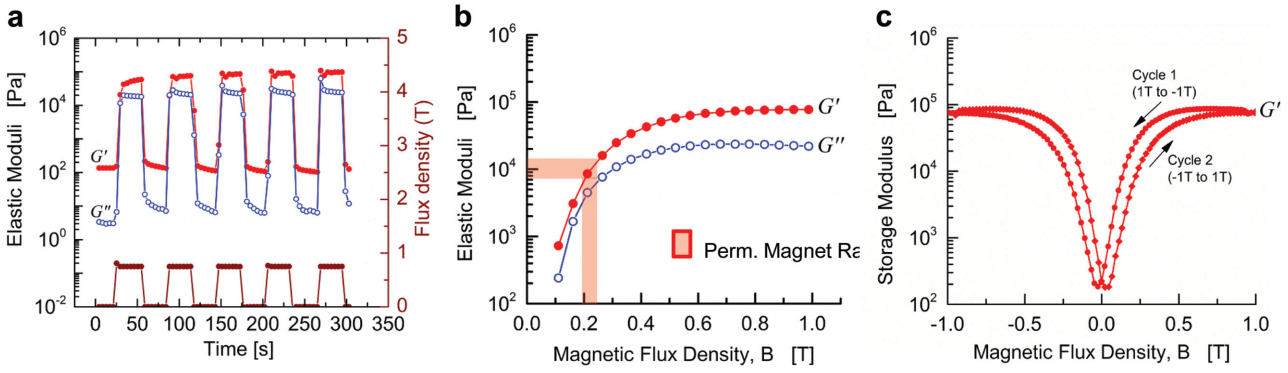

Figure 2. Magnetic field dependent elasticity of PA-CI gels. a) Pulsed magnetic field from 0 to 0.75 T showing three orders of magnitude change to elasticity. b) A magnetic field ramp showing a continuous rise in the modulus with field strength, with the highlighted region representing magnetic flux density achieved with permanent magnets. c) Elastic hysteresis is observed between back and forth ramps from –1 to 1 T.

maintaining its configuration from a previous cycle (cycle 1, from 0 to –1 T), and rearranging to a different configuration in cycle 2 when the field was being ramped up from 0 to 1 T.

Next, we checked the particle fraction dependence of the composite (Figure S4, Supporting Information). At magnetic field (B) = 0 T, the linear elastic modulus (G') shows no frequency dependence for all considered concentrations and the loss modulus (G'') shows weak frequency dependence before being affected by instrument rotational inertia, shown as a limit line in the figure.[47] Up to a volume fraction of 30% in the composite, both moduli increase with increasing particle concentration, beyond which the composite elasticity drops with particle inclusion, and the gel degrades. The magnetic field dependent mechanical properties of each resulting composite are outlined (Figure S4b, Supporting Information), and serve as a good reference for the choice of 30% particle volume fraction in the gel, which represents the maximum change in G'.

To determine the effect of the surface functionality on treated/untreated CI particles in the composite, we studied the magnetic field dependent mechanical properties of untreated and amine-treated particles in the polyacrylamide gel (Figure S5, Supporting Information). The linear viscoelastic properties of the composite show no significant difference when compared to the properties of the composite with untreated particles. Both moduli show strong magnetic field dependence (Figure S5b, Supporting Information) and increase ~100× as the field is ramped from 0 to 1 T. The same material is then exposed to five cycles of a pulsed magnetic field from 0 to 0.75 T (Figure S5c, Supporting Information). The linear viscoelastic moduli are reversible between cycles 2 and 5 and show ~200× increase in moduli. A larger relative change in moduli here is attributed to a faster rate of change of magnetic field, in contrast to a slow and gradual growth from 0 to 1 T in the ramps shown in Figure S5b (Supporting Information). A study with methacrylate treated particles in the gel was also attempted, but consistently resulted in a heterogeneous composite that showed noticeable phase separation at the volume fractions of interest, $\phi = 30\%$.

As a control with particles alone, we formulated a suspension of amine-treated carbonyl particles in a silicone oil-grease medium (Figure S6, Supporting Information). This medium has a low yield stress of ~2 Pa which inhibits particle sedimentation for ~24 h.[48] The storage modulus and loss modulus increase with increasing particle volume fraction. We show this volume fraction dependence with a characteristic shear modulus $G_0 \equiv G'(\omega = 1 \text{ rad s}^{-1})$, both with and without magnetic field (Figure S6b, Supporting Information). The suspension shows magnetic field dependent linear viscoelasticity that scales as $G_0 \approx \phi^{2.2}$, an exponent that is slightly larger than the earlier observed scaling of 1.7.[49]

While tunability across the entire range of elasticity is desirable, the equipment used to impose a variable magnetic field is expensive, requires electrical power, and is cumbersome in cell culture environments. An alternate solution is to use permanent magnets which can provide a constant magnetic field, which can be changed by varying the distance between magnet and gel. We used permanent rare earth magnets attached to a well plate cover (**Figure 3**, inset), upon which the hydrogel samples with cells in well plates can be placed. By measuring the magnetic field strength using a Hall probe, we found the field

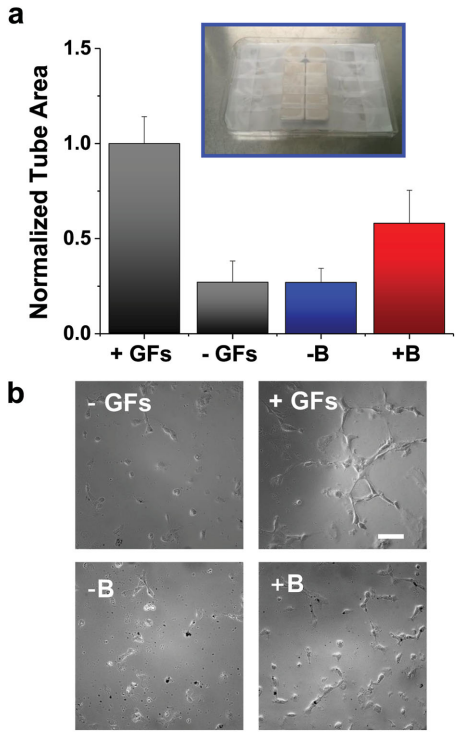

Figure 3. Stiffening hydrogels enhances secretion of proangiogenic factors. a) HMVEC tube formation on matrigel is quantified as a function of secreted factors in the conditioned medium. Conditioned medium is obtained from MSCs cultured on magnetoactive hydrogels cultured with and without a magnetic field. EGM-2 media is used as a positive control (+ GFs) and unconditioned DMEM is used as a negative control (- GFs). (Inset) Permanent rare earth magnets taped to the underside of a well plate cover. Well plates with samples inside them can be placed on top of this well plate cover to introduce a magnetic field to substrates. b) Representative images of tube formation on the positive control, negative control, and with or without magnetic field conditions (scale bar: 100 μm). Error bars represent standard error.

to be ~0.2–0.25 T which corresponds to a storage modulus in the range ~8–15 kPa. (Figure 2b) Therefore, with this setup, we can "switch" or "oscillate" the modulus between 0.1 and 0.14 Pa (no magnet) and 8–15 kPa (with magnet). Henceforth these will be given the designations "soft" and "stiff," respectively.

2.3. Modulation of Substrate Stiffness Guides Secretion of Proangiogenic Molecules, Cell Spreading, and Differentiation

Previously, we demonstrated how increasing stiffness of fibronectin conjugated hydrogels will enhance MSC proangiogenic potential.[17] First, to confirm protein incorporation onto the magnetoactive gel surfaces we used fluorescently tagged fibronectin and confirmed increased fluorescence signal from the hydrogels after addition (Figure S7a, Supporting Information). Next, we micropatterned fibronectin on our gel surface using a polydimethylsiloxane (PDMS) stamp fabricated through photolithography to present oval features in relief. After addition of MSCs, we observe preferential adhesion to the micropatterned regions (Figure S7b, Supporting Information). We also tested the effect of magnetic fields on protein arrangement on

the gel surface (Figure S8, Supporting Information). Fluorescence analysis indicates negligible changes in the uniformity; however, direct gel contact with the magnet leads to the appearance of fluorescent lines suggesting some adhesion to the particles within the gel that becomes apparent after alignment in a magnetic field.

We cultured MSCs on our tunable hydrogel for 2 days and performed a tube formation assay (human microvascular endothelial cells (HMVECs) on matrigel as described previously[17]) using the conditioned medium from MSCs cultured on the surfaces with (+*B*) or without (−*B*) a magnetic field. We also used endothelial growth media-2 (EGM-2) as a positive control and unconditioned Dulbecco's Modified Eagle medium (DMEM) as a negative control. Quantifying the tube area from the different media (Figure 3) shows almost double the tube formation for MSCs cultured on stiff versus soft surfaces. This trend agrees with our expectations for MSCs on soft or stiff substrates and demonstrates the potential for using dynamic magnetoactive materials to guide angiogenesis when MSCs are a therapeutic agent.

To further investigate how changing the elasticity in vitro will influence adherent cells, we used one of the fastest "cellular indicators" of substrate elasticity: cell spread area. Cell spread area generally increases with substrate stiffness and the changes happen relatively quickly. We cultured MSCs on soft and stiff conditions for 4 h and then we switched a subset of the MSCs from stiff to soft and cultured them for a further 4 h (**Figure 4**a). Overall, MSCs on soft substrates had an average area of about 750 μm^2 while those on stiff substrates had an average area of ≈1300 μm^2 (Figure 4b). Cells cultured on stiff-to-soft substrates reverted to an area of ≈900 μm^2, just above that from soft substrates. Interestingly, some cells showed more prominent actin staining when cultured on stiff versus soft substrates which persisted for 4 h (Figure 4a, bottom). Taken together, this shows that reversible changes in substrate stiffness can lead to reversible changes in cellular spreading.

MSC osteogenesis is another important bioactivity that has been studied extensively on hydrogels.[12,17,50] Generally, going to stiffer substrates increases osteogenic marker expression. Runx2 is an important transcription factor involved in regulating lineage specification, and is the most common marker used to classify early osteogenesis. Several reports have demonstrated a "memory effect" where the properties of a previous microenvironment influences cell state to a degree that lineage-specific activity remains apparent.[25,26,34] Guvendiren and Burdick show a dependence of Runx2 expression when gels are switched from soft-to-stiff at different time points, with gels switched earlier showing increased Runx2 expression.[34] We performed a similar experiment with MSCs cultured on soft, stiff, or switched from soft-to-stiff. First, cells were seeded and allowed to attach for 1 d at one stiffness, then the stiffness was changed at day 2, and again at day 5 (**Figure 5**a, left). We then imaged and quantified Runx2 expression at 10 d (Figure 5b). The experiment was performed in this way in order to see the relative effects of stiffness changes during cell attachment and spreading (up to day 2) and in the early (up to day 5) and late stages (days 5–10) of our study of early osteogenic lineage specification. We used six different variations labeled with H for high stiffness and L for low stiffness (e.g., HLH indicates high

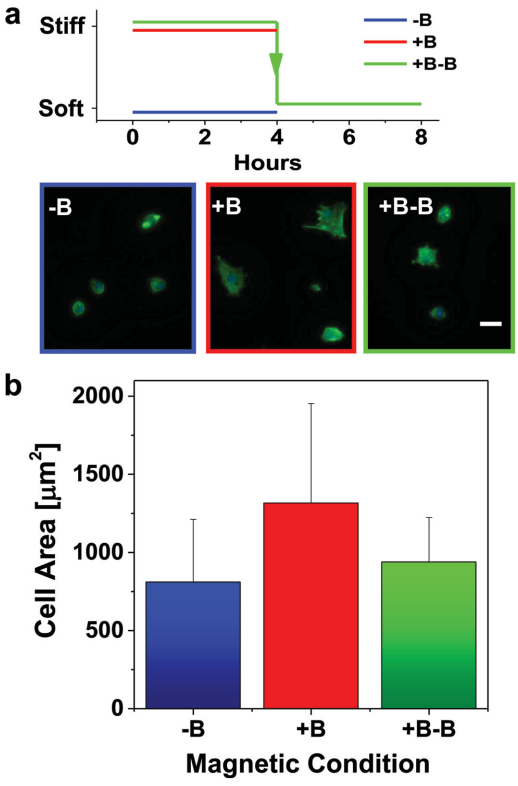

Figure 4. Modulating hydrogel stiffness in vitro reversibly affects MSC spread area. a) (Top) Cells were cultured with (+B) or without (−B) a magnetic field or cultured for 4 h on a magnetic field and then the field was switched off (+B–B). (Bottom) Representative images of MSCs cultured on these substrates at these different conditions (Scale bar: 50 μm). b) Quantification of average MSC area.

stiffness for 1 d, low stiffness for 4 d, and high stiffness for the remaining 5 d). To highlight relative differences between samples, the data are shown as deviation of Runx2 expresssion from the average of all samples at day 10. Analysis of Runx2 expression indicates that initial stiffening plays a significant role in guiding the final differentiation state. Furthermore, stiffness condition during the later stages of culture (last 5 d) corresponded with the largest increase in Runx2 intensity. Surprisingly, intermediate stiffening (between days 2 and 5) did not exert a significant influence on Runx2 expression.

Interestingly, after 10 d the average cell area was similar between the soft and stiff conditions (Figure S9a, Supporting Information). This result is somewhat surprising, and may be related to cells adapting a preferred shape after differentiation, or through remodeling their microenvironment and the hydrogel properties. Nevertheless, looking at cell area versus Runx2 expression for a random sample of 200 cells (Figure S9b, Supporting Information) we observed that for virtually any particular range of areas, Runx2 expression was higher in cells on stiff matrices when compared to soft.

3. Discussion

We have demonstrated a magnetically tunable hydrogel system, using functionalized carbonyl iron particles in a polyacrylamide

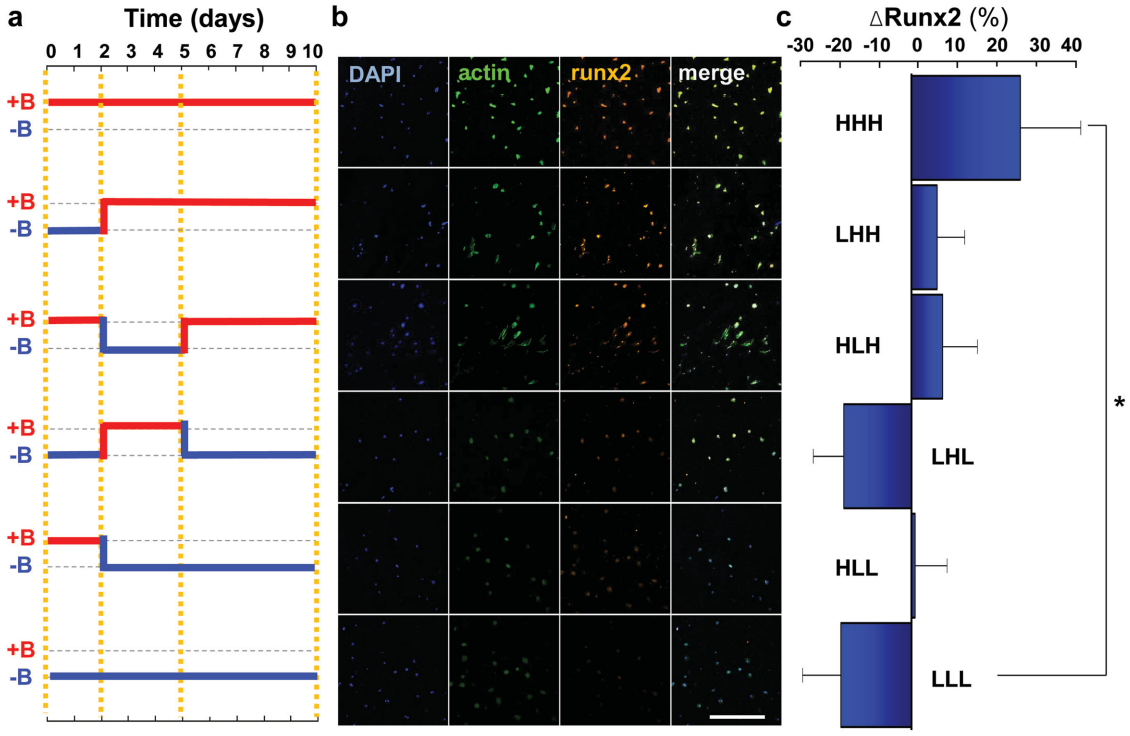

Figure 5. Dynamic stiffening guides the extent of osteogenesis in mesenchymal stem cells. a) Magnetization profile for dynamic stiffening in culture. b) Representative images of DAPI, Phalloidin, and Runx2 of MSCs cultured for 10 d at various magnetic field profiles, with (+B) or without (–B) magnetic fields (scale bar: 500 μm). c) Percent change of Runx2 expression (compared to average of all samples at day 10) in MSCs cultured for 10 d in bipotential osteogenic/adipogenic medium at different magnetic field profiles from the overall average. $*P < 0.05$.

matrix, which shows a several-fold change in elasticity when subjected to magnetic fields. The CI particles reinforce the gel at higher magnetic fields, increasing elasticity reversibly. The CI particles can be modified by flexible silane chemistries for conjugation to the polymer network or other moieties. Using a magnetic field as a stimulus has the added benefit of not affecting cellular cycle and growth which has been shown for fields up to 10 T.[51]

Mechanical characterization shows possible modulation of storage modulus between ~0.1 and ~80 kPa reversibly. This accessible range of elasticities can cover most of the physiologically relevant tissue stiffness giving this platform wide applicability as a model system for studying mechanical effects on different cellular systems in vitro.

We show how simple and inexpensive permanent magnets can be used to dynamically stiffen hydrogels for the investigation of several cellular activities that are influenced by mechanical properties. Although this approach sacrifices the ability to continuously tune the elasticity, it allows switching between soft and stiff conditions and retains the reversibility. It is important to consider that, with particle alignment, there are some changes in protein distribution and changes in surface topography and alignment may also occur that modulate cell behavior or adhesion.[40] MSCs cultured on soft substrates show nearly a twofold increase in spread area when a magnet is applied. The influence on cell area is reversible and the cell area is reduced after removal of the magnet; curiously however, stained actin remains brighter in cells cultured on magnetically treated gels compared to cells cultured on soft gels without an applied field. This may be related to residual "stiffening" effects caused by hysteresis we observed when magnetic fields are removed.

Using this simplified system, we show that the proangiogenic potential of MSCs increase when they are cultured on magnetically stiffened substrates, which agrees with our previous observations on static polyacrylamide hydrogels. In addition to proangiogenic secretion, we show how the degree of MSC osteogenesis can be dynamically modulated by simply adding or removing a magnet below the culture plate. After 10 d exposure to differentiation promoting media, MSCs cultured on magnetoactive hydrogels display susceptibility to the temporal dynamics of stiffening. MSCs initially seeded on a stiff matrix appear predisposed to osteogenesis, while initial seeding on soft matrices appears to discourage lineage commitment. Interestingly, stiffening during intermediate times in our experiment (days 2–5) did not enhance osteogenesis compared to MSCs cultured on soft gels for the entire experiment. Stiffening at later timepoints (days 5–10) exerted a larger influence on osteogenesic marker expression at 10 d. Notably, since we are evaluating Runx2 expression through immunofluorescent staining, accumulation of protein with time plays a role, giving extra weight to total time spent at each stiffness condition, perhaps explaining why the HHH condition shows higher protein expression than the LHH or HLH conditions. Overall, we speculate that mechanotransduction during early stages of culture are important for initiation of osteogenic signaling. This is consistent with previous reports of early mechanical signals promoting a susceptibility to the osteogenesis program.[25]

4. Conclusion

The dynamic modulation of stem cell activity using magnetic fields demonstrates the potential of this system for studying temporal regulation of ECM mechanical properties in physiological and pathological contexts, adding tunable stiffness to other applications of magnetoactive hydrogels in tissue engineering such as on-demand drug and cell delivery[52] and modulation of surface roughness and topography.[53] To our knowledge, there has only been one other study where magnetoactive hydrogels have been used in cell culture,[40] and then with PDMS elastomer. Our study here facilitates bridging the gap between the need for tunable hydrogels for cell culture and magnetoactive systems to study dynamic microenvironments. Some examples of dynamic microenvironments observed in vivo include gastrulation,[54] branching morphogenesis,[55] cardiovascular development and function,[56] and pathophysiological processes such as fibrosis and cancer.[22,57] Although the use of permanent magnets is convenient, more advanced magnetic accessories will be necessary to capture subtle changes underlying many biological processes. Nevertheless, this simple technique for studying the effect of dynamic temporal modulation of substrate mechanics on cell activity, that is flexible enough to be used in many different hydrogel platforms, may find broad applicability for cell biology studies and for "priming" cells to an appropriate state for therapy.

5. Experimental Section

All materials were bought from Sigma-Aldrich unless otherwise noted.

CI Particle Modification and Hydrogel Preparation: CI particles (grade EW) were generously provided by QED Technologies. The particles were either amino functionalized using aminopropyl trimethoxysilane or methacrylate functionalized using 3-(trimethoxysilyl)propyl-methacrylate. The treatment was performed by incubating the particles in the desired silane dissolved in a 90% ethanol solution overnight under shaking. Modified CI particles were washed thoroughly with deionized (DI) water at least four times before use.

For gel preparation, a prepolymer solution mixture of acrylamide and bis-acrylamide (Fisher Scientific) was mixed according to the desired crosslinking density (here we used 3% acrylamide and 0.06% bis-acrylamide) and degassed under argon gas for 10 min. 18 mm glass coverslips were cleaned by sonication under ethanol for 15 min followed by sonication in DI water for 15 min. Coverslips were activated for gel attachment by treatment with 0.5% solution of APTES for 3 min followed by thorough washing with DI water three times. Coverslips were then treated with 0.5% glutaraldehyde solution for 30 min and washed with DI water. A hydrophobic microscope slide was prepared by treatment with Rain-X (SOPUS).

The desired mixture of CI particles by volume was prepared in prepolymer solution. Gelation was initiated by addition of 0.1% ammonium persulfate and 0.1% tetramethylethylenediamine and vortexing the solution. 20 µL of solution was pipetted onto the hydrophobic microscope slide and the activated coverslip was placed face down on the drop. The gel was left to solidify for ~20 min and was then detached from the hydrophobic slide. Gels were washed at least three times with DI water to remove any particles not incorporated during gelation.

For protein incorporation, fibronectin (from human plasma) at 50 µg mL^{-1} was incubated on the surface of PDMS stamps for 30 min. Then, air was used to blow excess solution from the surface of the PDMS stamps and fibronectin was transferred to the surface of the gel by stamping. Gels were washed several times in DI water and stored in 12-well plates until cell culture.

SEM: SEM images of dried PA hydrogels with modified CI particles were acquired using a JEOL 6060-LV scanning electron microscope under high vacuum. A thin layer of gold was sputtered onto the surfaces to ensure electrical conductivity of the samples. Images were taken at either 1000× or 3500×.

Fourier Transform Infrared Spectroscopy (FTIR): FTIR was performed on a Spectrum 100 (Perkin Elmer) machine in transmittance mode. Spectra were taken at each point between 450 and 4000 cm^{-1} on samples in dichloromethane on a potassium bromide salt plate. Baseline correction and normalization were performed on spectra.

Mechanical Characterization: Dynamic shear measurements were performed on a rotational rheometer (combined-motor-transducer, DHR-3, TA Instruments) with a magnetorheology (MR) setup for uniform and controlled application of magnetic fields from –1 to +1 T (experimental setup shown in Figure S2a, Supporting Information). Disks of samples of 1 mm thickness and 20 mm diameter were prepared, and measurements were made with a nonmagnetic 20 mm diameter parallel plate fixture. An electromagnetic coil beneath the sample imposed magnetic field lines orthogonal to the plate surface, and a hall probe under the bottom fixed plate gave real time measurement of the external field strength during tests. An upper yoke surrounded the upper geometry to draw field lines orthogonal to the plate surfaces. Tests were run at a constant temperature of 37 °C, maintained by a closed-loop-control fluid circulator through the bottom MR fixture. For experiments performed in the presence of a magnetic field, oscillations were run at a frequency of 1 rad s^{-1} and shear strain amplitude of 1% (in the linear viscoelastic regime).

Cell Culture: Human MSCs were purchased and tested for purity from Lonza and were positive for CD105, CD166, CD29, and CD44 and negative for CD14, CD34, and CD45 by flow cytometry. HMVECs were purchased from Cell Systems. EGM-2-supplemented media was purchased from Lonza. The use of human cell lines in this work was reviewed and approved by the University of Illinois at Urbana–Champaign Biological Safety Institutional Review Board.

MSCs were cultured in low glucose DMEM supplemented with 10% fetal bovine serum and 1% penicillin/streptomycin. HMVECs were cultured in EGM-2 on attachment factor (Life Technologies). Media was changed every 3–4 d and cells were passaged at ~80% confluence. Cells were seeded on surfaces at passages 3–7.

For differentiation experiments, MSCs were cultured for 10 d in mixed (1:1) bipotential adipogenic/osteogenic differentiation media (Lonza) as per the manufacturer's instructions.

Tube Formation Assay: Vascularization assays were performed with MSC conditioned media as described previously.[17] Briefly, growth-factor-reduced basement membrane (matrigel, Trevigen) was coated on the bottom surfaces of a 48-well plate and gelled at 37 °C for 30 min. HMVECs were seeded onto the matrigel at ≈15 000 cells per well in serum and growth factor free media (EBM-2, Lonza) and conditioned media from MSCs cultured at different conditions was added. After 8 h, tube formation was imaged using a Rebel DSLR camera (Canon) and tube area quantified using ImageJ (NIH).

Immunostaining: Surfaces were rinsed twice with phosphate buffered saline and were then fixed with 4% paraformaldehyde for 20 min.

Surfaces were permeabilized for 30 min in 0.1% Triton X-100 and then blocked in 1% bovine serum albumin for 1 h. Runx2 was stained with a primary rabbit-anti-Runx2 (ABCAM) overnight at 4 °C and secondary 555-Alexa fluor goat anti-rabbit antibody (1:200) (Invitrogen). Actin and nuclei were stained by Alexa-Fluor 488-phalloidin (1:200) and 4,6-diamidino-2-phenylindole (DAPI; 1:5000), respectively. Secondary staining was performed for 20 min at 37 °C.

Fluorescence Imaging and Data Analysis: Immunostained cells were imaged using a Zeiss Axiovert inverted fluorescence microscope (Carl Zeiss) or an IN Cell Analyzer 2000 (General Electric). Cell area was measured from phalloidin staining of the actin cytoskeleton using ImageJ and nuclear Runx2 intensity was measured using DAPI as a mask for nuclei. Runx2 intensity was reported as nuclear intensity minus cytoplasmic intensity. Statistical significance was determined using two-tailed *p*-values from unpaired *t*-test for comparing two groups. Error bars represented standard error.

Supporting Information

Supporting Information is available from the Wiley Online Library or from the author.

Acknowledgements

A.A.A., N.A.B., R.H.E., and K.A.K. conceived the ideas and designed the experiments. A.A.A., J.L., and N.A.B. conducted the experiments and A.A.A., J.L., N.A.B., R.H.E., and K.A.K. analyzed the data. A.A.A., J.L., N.A.B., R.H.E., and K.A.K. interpreted the data and wrote the manuscript. This work was supported by the National Heart Lung and Blood Institute of the National Institutes of Health, grant number HL121757. The authors declared no competing financial interests.

Received: April 5, 2016
Revised: April 25, 2016
Published online: June 8, 2016

[1] M. E. Lukashev, Z. Werb, *Trends Cell Biol.* **1998**, *8*, 437.
[2] J. K. Mouw, G. Ou, V. M. Weaver, *Nat. Rev. Mol. Cell Biol.* **2014**, *15*, 771.
[3] V. Vogel, M. Sheetz, *Nat. Rev. Mol. Cell Biol.* **2006**, *7*, 265.
[4] A. Mammoto, T. Mammoto, D. E. Ingber, *J. Cell Sci.* **2012**, *125*, 3061.
[5] D. E. Discher, P. Janmey, Y.-L. Wang, *Science* **2005**, *310*, 1139.
[6] J. D. Humphrey, E. R. Dufresne, M. A. Schwartz, *Nat. Publ. Gr.* **2014**, *15*, 802.
[7] F. M. Watt, W. T. S. Huck, *Nat. Rev. Mol. Cell Biol.* **2013**, *14*, 467.
[8] F. Rosso, A. Giordano, M. Barbarisi, A. Barbarisi, *J. Cell. Physiol.* **2004**, *199*, 174.
[9] B. D. Hoffman, C. Grashoff, M. A. Schwartz, *Nature* **2011**, *475*, 316.
[10] K. S. Kolahi, M. R. K. Mofrad, *Wiley Interdiscip. Rev.: Syst. Biol. Med.* **2010**, *2*, 625.
[11] D. E. Jaalouk, J. Lammerding, *Nat. Rev. Mol. Cell Biol.* **2009**, *10*, 63.
[12] A. J. Engler, S. Sen, H. L. Sweeney, D. E. Discher, *Cell* **2006**, *126*, 677.
[13] J. Lee, A. A. Abdeen, D. Zhang, K. A. Kilian, *Biomaterials* **2013**, *34*, 8140.
[14] K. A. Kilian, B. Bugarija, B. T. Lahn, M. Mrksich, *Proc. Natl. Acad. Sci. USA* **2010**, *107*, 4872.
[15] J. Lee, A. A. Abdeen, X. Tang, T. A. Saif, K. A. Kilian, *Biomaterials* **2015**, *69*, 174.
[16] J. Lee, A. A. Abdeen, A. S. Kim, K. A. Kilian, *ACS Biomater. Sci. Eng.* **2015**, *1*, 218.
[17] A. A. Abdeen, J. B. Weiss, J. Lee, K. A. Kilian, *Tissue Eng., Part A* **2014**, *20*, 2737.
[18] F. P. Seib, M. Prewitz, C. Werner, M. Bornhäuser, *Biochem. Biophys. Res. Commun.* **2009**, *389*, 663.
[19] A. J. Engler, M. A. Griffin, S. Sen, C. G. Bönnemann, H. L. Sweeney, D. E. Discher, *J. Cell Biol.* **2004**, *166*, 877.
[20] K. Saha, A. J. Keung, E. F. Irwin, Y. Li, L. Little, D. V Schaffer, K. E. Healy, *Biophys. J.* **2008**, *95*, 4426.
[21] W. P. Daley, S. B. Peters, M. Larsen, *J. Cell Sci.* **2008**, *121*, 255.
[22] T. R. Cox, J. T. Erler, *Dis. Models Mech.* **2011**, *4*, 165.
[23] P. Lu, V. M. Weaver, Z. Werb, *J. Cell Biol.* **2012**, *196*, 395.
[24] P. M. Gilbert, K. L. Havenstrite, K. E. G. Magnusson, A. Sacco, N. A Leonardi, P. Kraft, N. K. Nguyen, S. Thrun, M. P. Lutolf, H. M. Blau, *Science* **2010**, *329*, 1078.
[25] C. Yang, M. W. Tibbitt, L. Basta, K. S. Anseth, *Nat. Mater.* **2014**, *13*, 645.
[26] J. Lee, A. A. Abdeen, K. A. Kilian, *Sci. Rep.* **2014**, *4*, 5188.
[27] X. Gaeta, Y. Xie, W. E. Lowry, *Nat. Cell Biol.* **2013**, *15*, 725.
[28] P. Y. Mengsteab, K. Uto, A. S. T. Smith, S. Frankel, E. Fisher, Z. Nawas, J. Macadangdang, M. Ebara, D.-H. Kim, *Biomaterials* **2016**, *86*, 1.
[29] O. Chaudhuri, L. Gu, D. Klumpers, M. Darnell, S. A. Bencherif, J. C. Weaver, N. Huebsch, H. Lee, E. Lippens, G. N. Duda, D. J. Mooney, *Nat. Mater.* **2016**, *15*, 326.
[30] J. A. Burdick, W. L. Murphy, *Nat. Commun.* **2012**, *3*, 1269.
[31] H. Y. Yoshikawa, F. F. Rossetti, S. Kaufmann, T. Kaindl, J. Madsen, U. Engel, A. L. Lewis, S. P. Armes, M. Tanaka, *J. Am. Chem. Soc.* **2011**, *133*, 1367.
[32] F. X. Jiang, B. Yurke, R. S. Schloss, B. L. Firestein, N. A. Langrana, *Biomaterials* **2010**, *31*, 1199.
[33] B. M. Gillette, J. A. Jensen, M. Wang, J. Tchao, S. K. Sia, *Adv. Mater.* **2010**, *22*, 686.
[34] M. Guvendiren, J. A Burdick, *Nat. Commun.* **2012**, *3*, 792.
[35] A. M. Kloxin, A. M. Kasko, C. N. Salinas, K. S. Anseth, *Science* **2009**, *324*, 59.
[36] A. M. Kloxin, M. W. Tibbitt, K. S. Anseth, *Nat. Protoc.* **2010**, *5*, 1867.
[37] A. M. Rosales, K. M. Mabry, E. M. Nehls, K. S. Anseth, *Biomacromolecules* **2015**, *16*, 798.
[38] A. M. Rosales, K. S. Anseth, *Nat. Publ. Gr.* **2016**, *1*, 1.
[39] T. Mitsumata, A. Honda, H. Kanazawa, M. Kawai, *J. Phys. Chem. B* **2012**, *116*, 12341.
[40] M. Mayer, R. Rabindranath, J. Börner, E. Hörner, A. Bentz, J. Salgado, H. Han, H. Böse, J. Probst, M. Shamonin, G. J. Monkman, G. Schlunck, *PLoS One* **2013**, *8*, e76196.
[41] T. Mitsumata, S. Ohori, A. Honda, M. Kawai, *Soft Matter* **2013**, *9*, 904.
[42] J. R. Tse, A. J. Engler, *Current Protocols in Cell Biology*, **2010**, John Wiley & Sons, Inc., Hoboken, NJ, Preparation of hydrogel substrates with tunable mechanical properties, *47*, 10.16, Ch. 10.
[43] B. Trappmann, J. E. Gautrot, J. T. Connelly, D. G. T. Strange, Y. Li, M. L. Oyen, M. A. C. Stuart, H. Boehm, B. Li, V. Vogel, J. P. Spatz, F. M. Watt, W. T. S. Huck, *Nat. Mater.* **2012**, *11*, 642.
[44] D. Lin-Vien, N. B. Colthup, W. G. Fateley, J. G. Grasselli, *The Handbook of Infrared and Raman Characteristic Frequencies of Organic Molecules*, **1991**, Elsevier Inc., Philadelphia, PA.
[45] C. Storm, J. J. Pastore, F. C. MacKintosh, T. C. Lubensky, P. A. Janmey, *Nature* **2005**, *435*, 191.
[46] J. de Vicente, D. J. Klingenberg, R. Hidalgo-Alvarez, *Soft Matter* **2011**, *7*, 3701.

[47] R. H. Ewoldt, M. T. Johnston, L. M. Caretta, Experimental challenges of shear rheology: how to avoid bad data, in *Complex Fluids in Biological Systems* (Ed: S. E. Spagnolie), Springer, New York **2015**, pp. 207–241.
[48] J. H. Park, M. H. Kwon, O. O. Park, *Korean J. Chem. Eng.* **2001**, *18*, 580.
[49] J. Claracq, J. Sarrazin, J. P. Montfort, *Rheol. Acta* **2004**, *43*, 38.
[50] A. S. Rowlands, P. A. George, J. J. Cooper-White, *Am. J. Physiol.: Cell Physiol.* **2008**, *295*, 1037.
[51] J. Miyakoshi, *Prog. Biophys. Mol. Biol.* **2005**, *87*, 213.
[52] X. Zhao, J. Kim, C. A. Cezar, N. Huebsch, K. Lee, K. Bouhadir, D. J. Mooney, *Proc. Natl. Acad. Sci. USA* **2011**, *108*, 67.
[53] J. D. Kiang, J. H. Wen, J. C. Del Álamo, A. J. Engler, *J. Biomed. Mater. Res., Part A* **2013**, *101 A*, 2313.
[54] A. Latimer, J. R. Jessen, *Matrix Biol.* **2010**, *29*, 89.
[55] H. Y. Kim, C. M. Nelson, *Organogenesis* **2012**, *8*, 56.
[56] M. Rienks, A. P. Papageorgiou, N. G. Frangogiannis, S. Heymans, *Circ. Res.* **2014**, *114*, 872.
[57] C. Bonnans, J. Chou, Z. Werb, *Nat. Rev. Mol. Cell Biol.* **2014**, *15*, 786.